

Supporting Information for

Fabrication of Ru Nanoclusters on Co-doped NiSe Nanorods with Efficient Electrocatalytic Activity towards Alkaline Hydrogen Evolution via Hydrogen Spillover Effect

Ce Mu, Hongqiang Xin, Qiaomei Luo, Yan Li* and Fei Ma*

State Key Laboratory for Mechanical Behavior of Materials, Xi'an
Jiaotong University, Xi'an, 710049, China

*E-mail address: mafei@mail.xjtu.edu.cn (Fei Ma)
 liyan0802@xjtu.edu.cn (Yan Li)

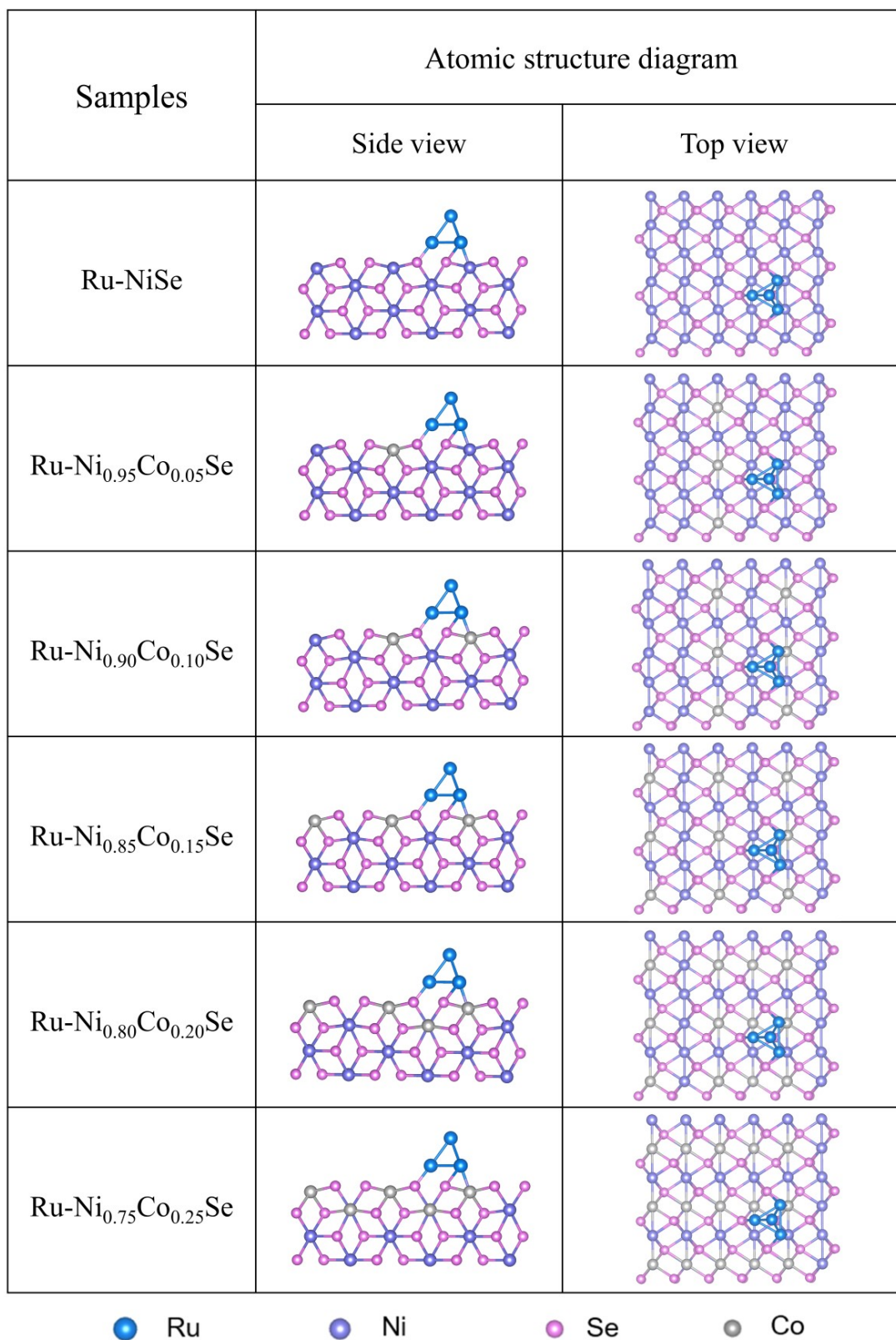


Figure S1. Atomic Structure diagram of different samples.

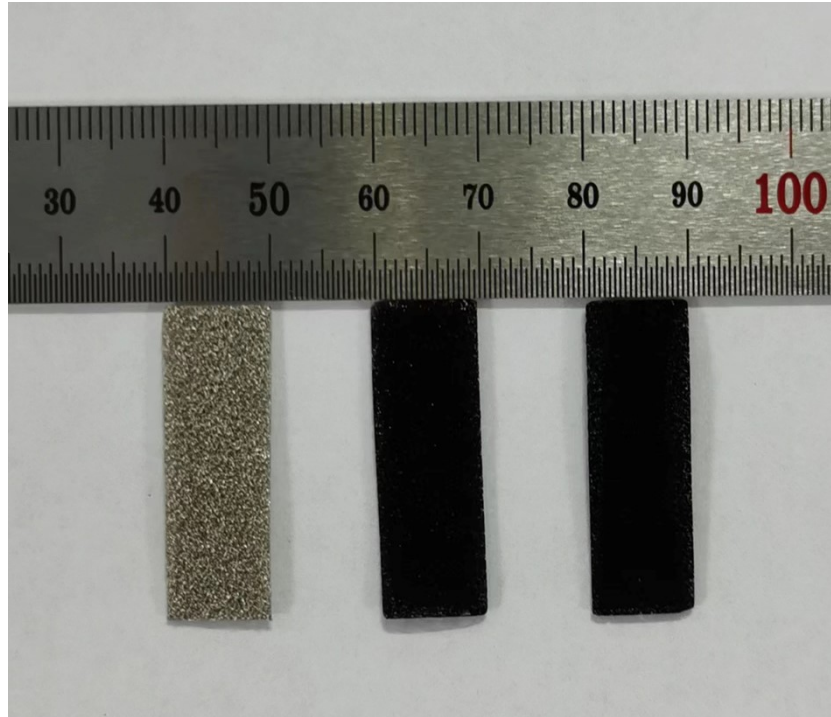


Figure S2. Photograph of blank Ni foam (left), NiSe NR/NF (mid) and Ru-Ni_{0.85}Co_{0.15}Se/NF (right).

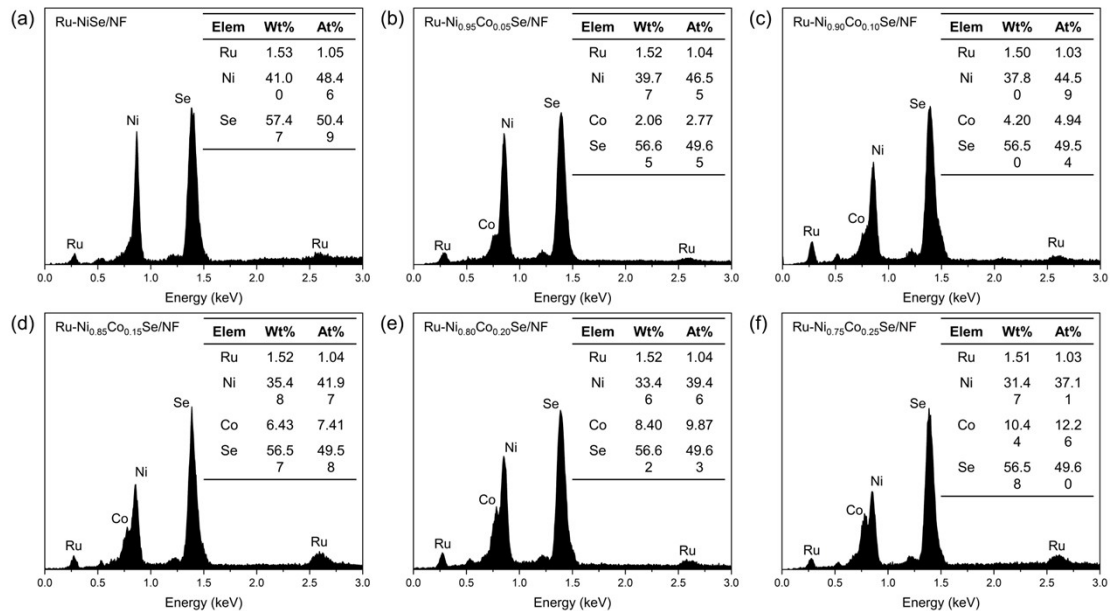


Figure S3. EDX spectra of (a) Ru-NiSe/NF, (b) Ru-Ni_{0.95}Co_{0.05}Se/NF, (c) Ru-Ni_{0.90}Co_{0.10}Se/NF, (d) Ru-Ni_{0.85}Co_{0.15}Se/NF, (e) Ru-Ni_{0.80}Co_{0.20}Se/NF and (f) Ru-Ni_{0.75}Co_{0.25}Se/NF.

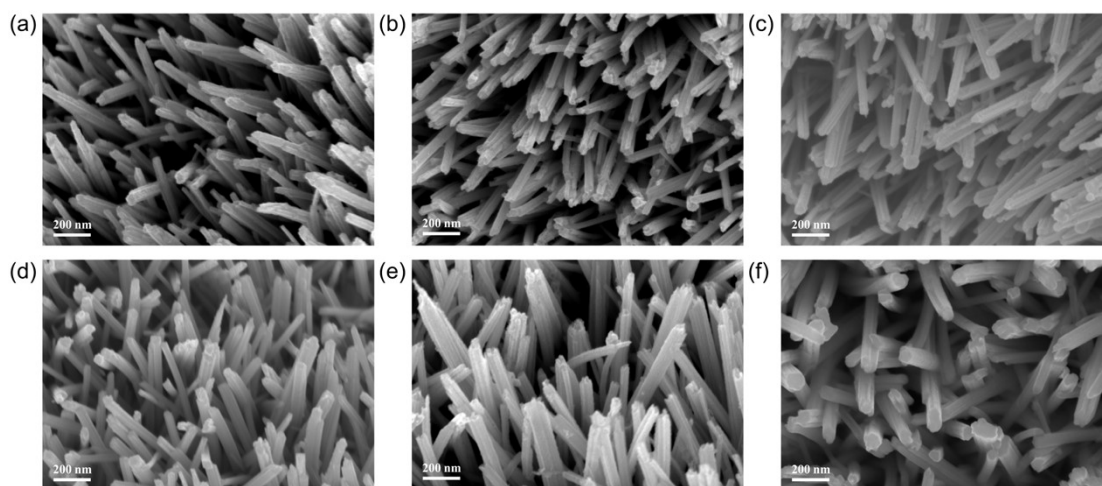


Figure S4. SEM images of (a) Ru-NiSe/NF, (b) Ru-Ni_{0.95}Co_{0.05}Se/NF, (c) Ru-Ni_{0.90}Co_{0.10}Se/NF, (d) Ru-Ni_{0.85}Co_{0.15}Se/NF, (e) Ru-Ni_{0.80}Co_{0.20}Se/NF and (f) Ru-Ni_{0.75}Co_{0.25}Se/NF.

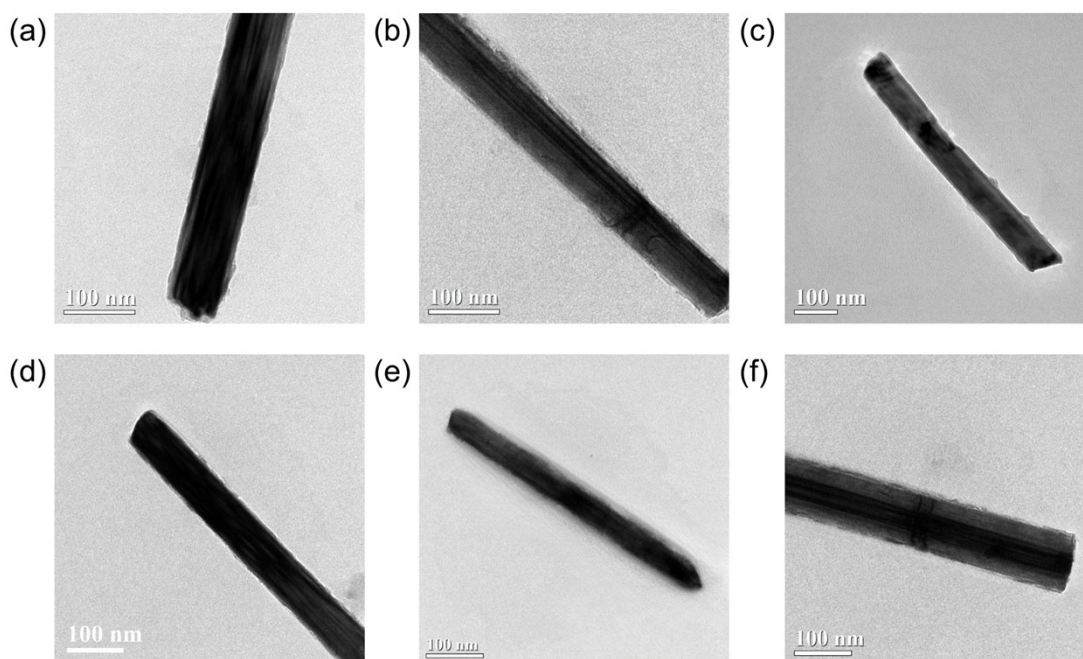


Figure S5. TEM images of (a) Ru-NiSe/NF, (b) Ru-Ni_{0.95}Co_{0.05}Se/NF, (c) Ru-Ni_{0.90}Co_{0.10}Se/NF, (d) Ru-Ni_{0.85}Co_{0.15}Se/NF, (e) Ru-Ni_{0.80}Co_{0.20}Se/NF and (f) Ru-Ni_{0.75}Co_{0.25}Se/NF.

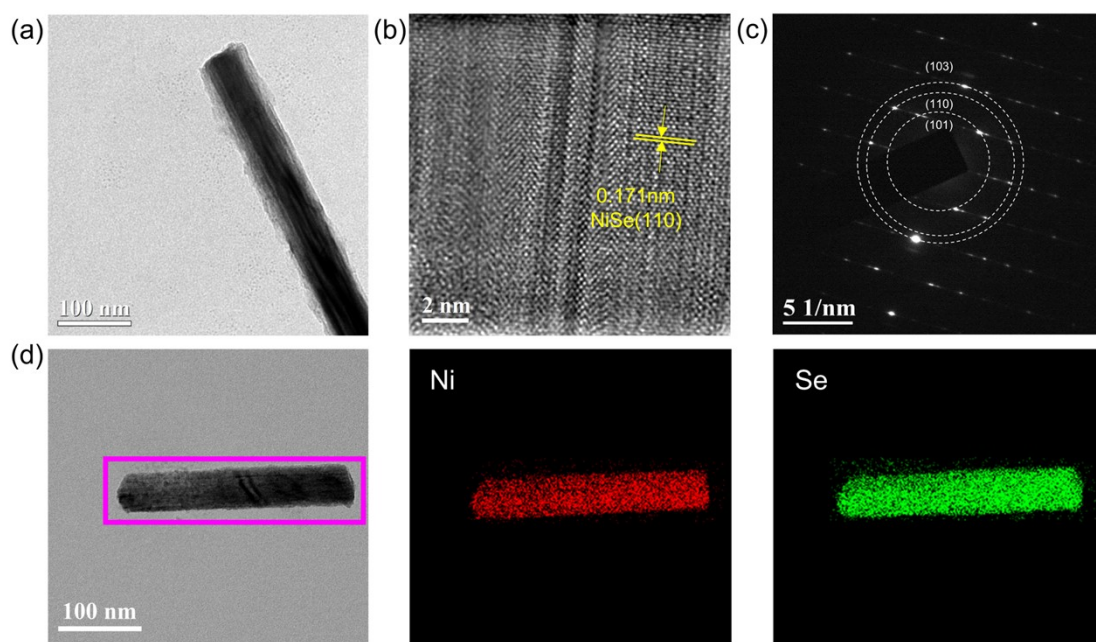


Figure S6. (a) TEM image, (b) HRTEM image, (c) SAED pattern, and (d) The high angle annular dark field-scanning transmission electron microscopy (HAADF-STEM) image and corresponding EDX elemental mapping images of an individual NiSe/NF.

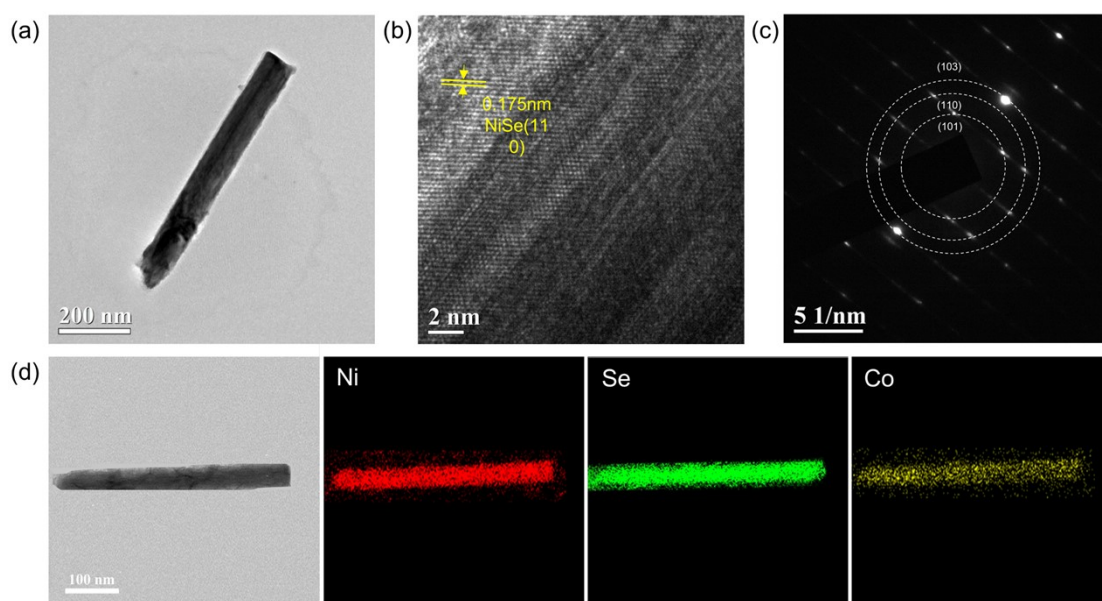


Figure S7. (a) TEM image, (b) HRTEM image, (c) SAED pattern, and (d) The high angle annular dark field-scanning transmission electron microscopy (HAADF-STEM) image and corresponding EDX elemental mapping images of an individual Ni_{0.85}Co_{0.15}Se/NF.

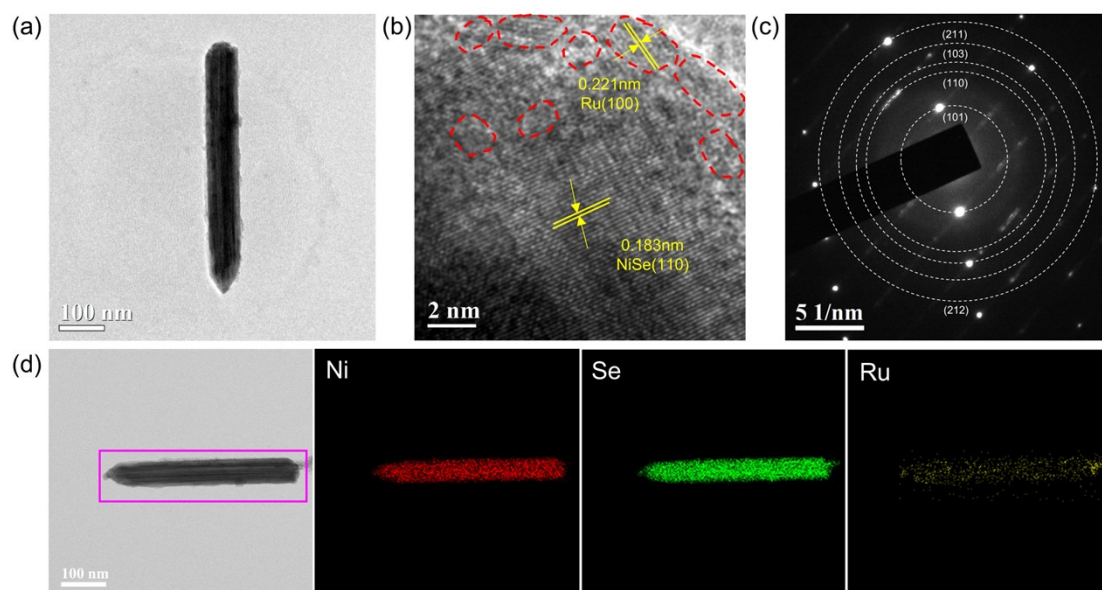


Figure S8. (a) TEM image, (b) HRTEM image, (c) SAED pattern, and (d) The high angle annular dark field-scanning transmission electron microscopy (HAADF-STEM) image and corresponding EDX elemental mapping images of an individual Ru-NiSe/NF.

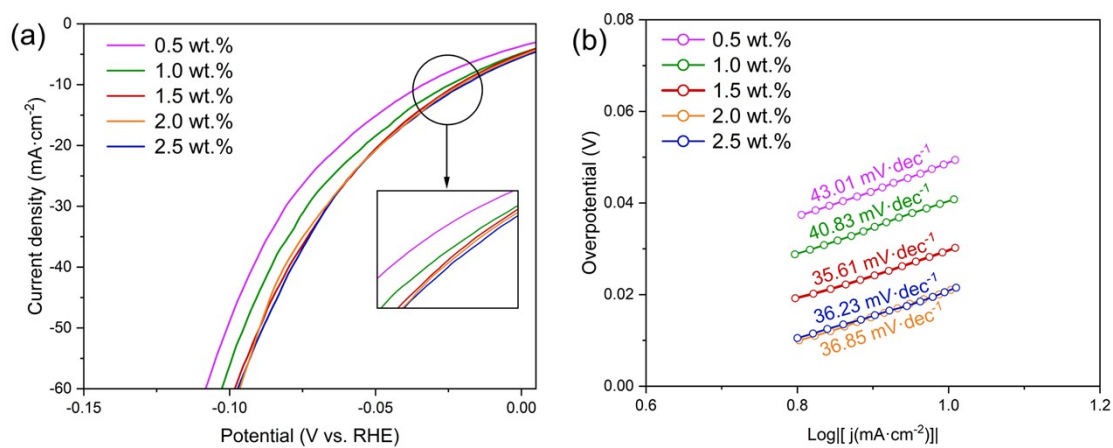


Figure S9. LSV curves and Tafel plots of the Ru-Ni_{0.85}Co_{0.15}Se/NF catalysts at different metal loading in 1.0 M KOH.

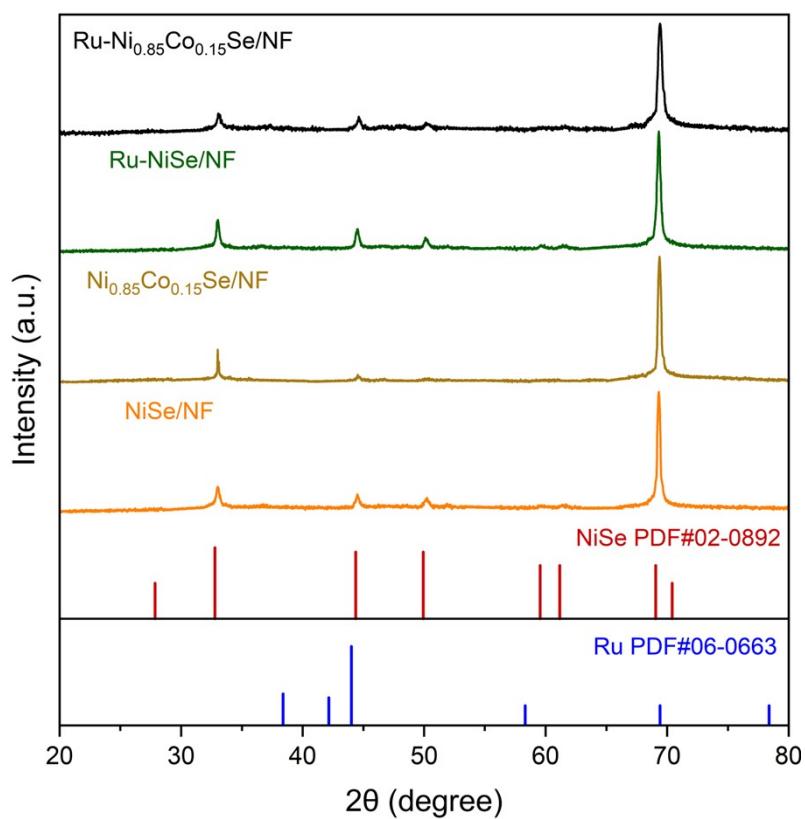


Figure S10. XRD patterns of NiSe/NF, Ru-NiSe/NF and Ru-Ni_{0.85}Co_{0.15}Se/NF.

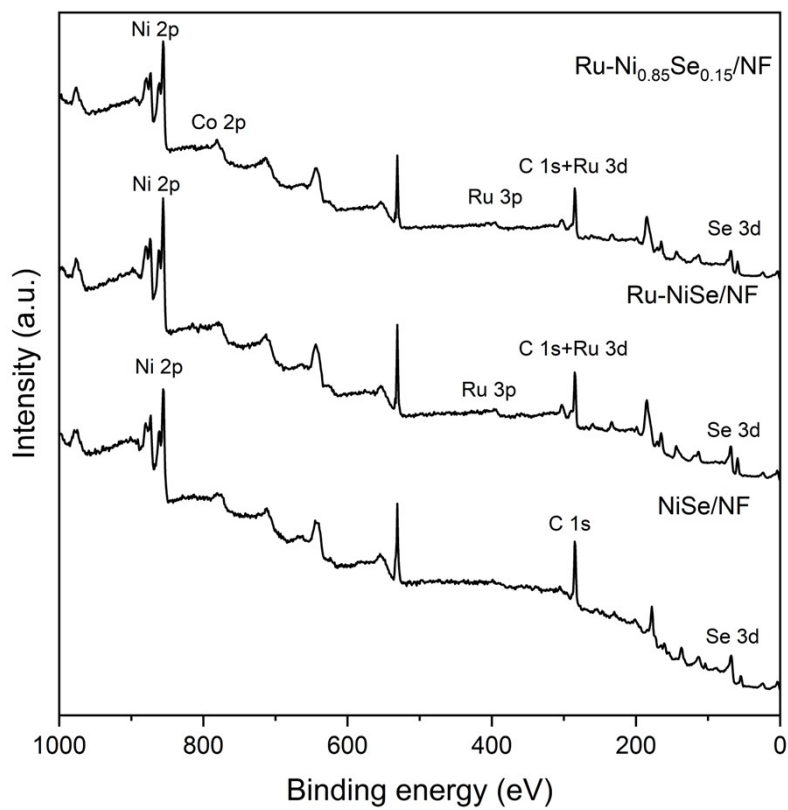


Figure S11. XPS spectra of NiSe/NF, Ru-NiSe/NF and Ru-Ni_{0.85}Co_{0.15}Se/NF.

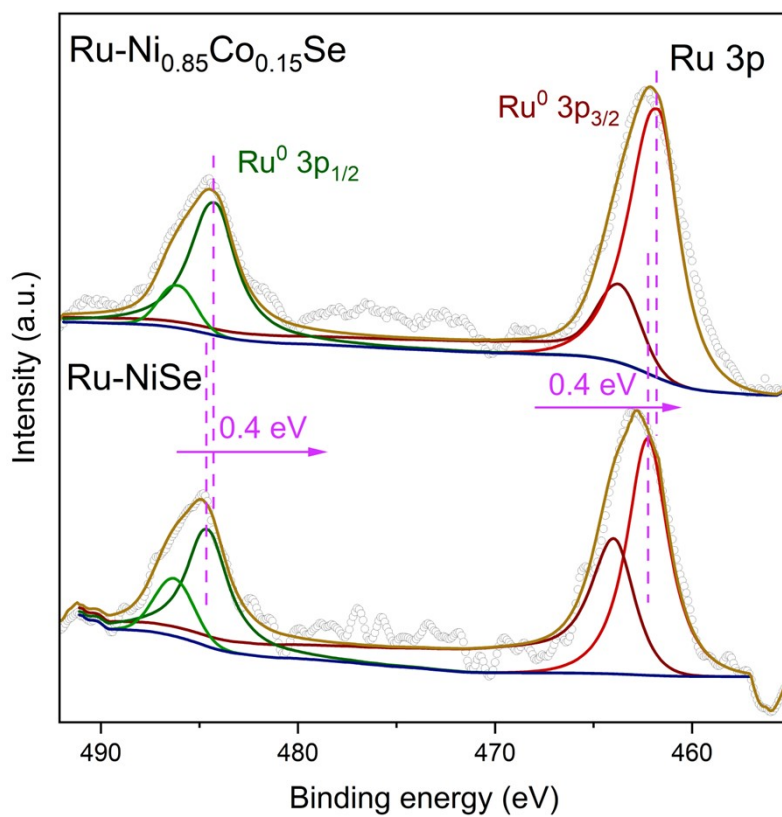


Figure S12. Ru 3p XPS spectra of Ru-NiSe/NF and Ru-Ni_{0.85}Co_{0.15}Se/NF.

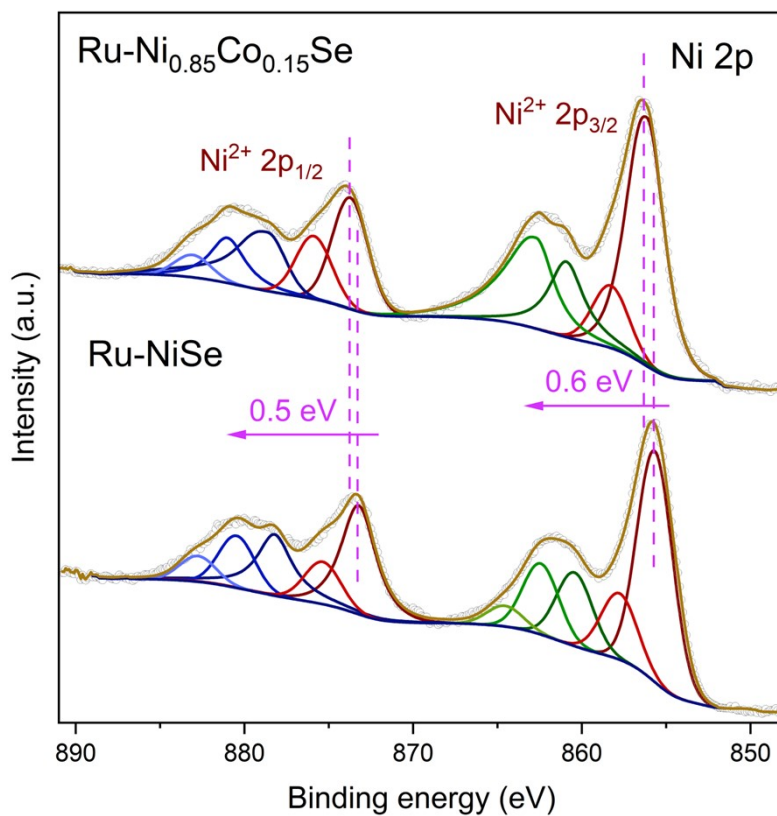


Figure S13. Ni 2p XPS spectra of Ru-NiSe/NF and Ru-Ni_{0.85}Co_{0.15}Se/NF.

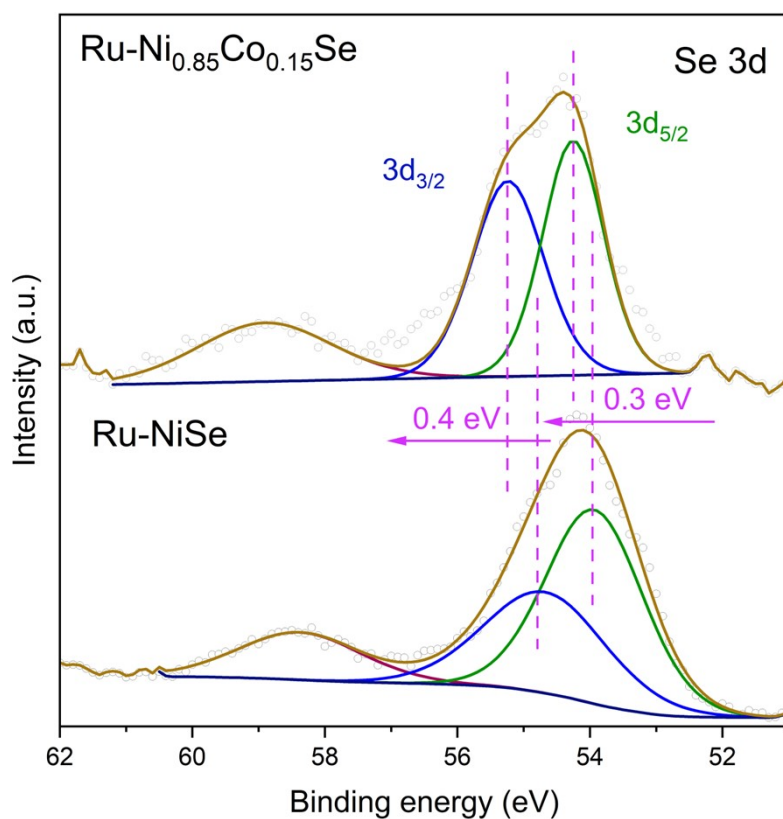


Figure S14. Se 3d XPS spectra of Ru-NiSe/NF and Ru-Ni_{0.85}Co_{0.15}Se/NF.

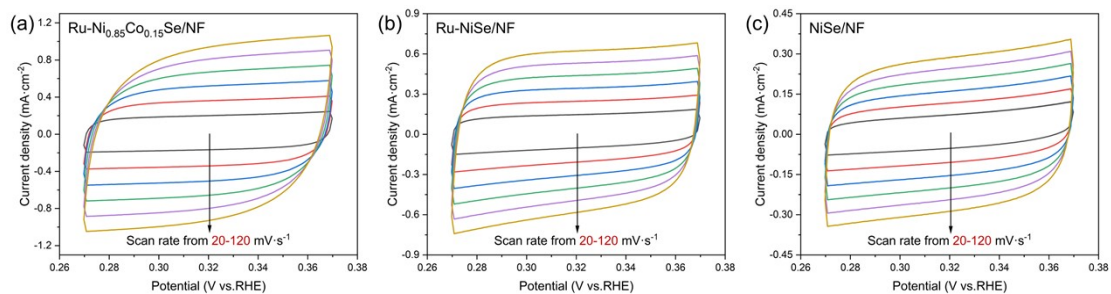


Figure S15. Cyclic voltammograms of (a)-(c) Ru-Ni_{0.85}Co_{0.15}Se/NF, Ru-NiSe/NF and NiSe/NF electrocatalysts in 1.0 M KOH at various scan rates.

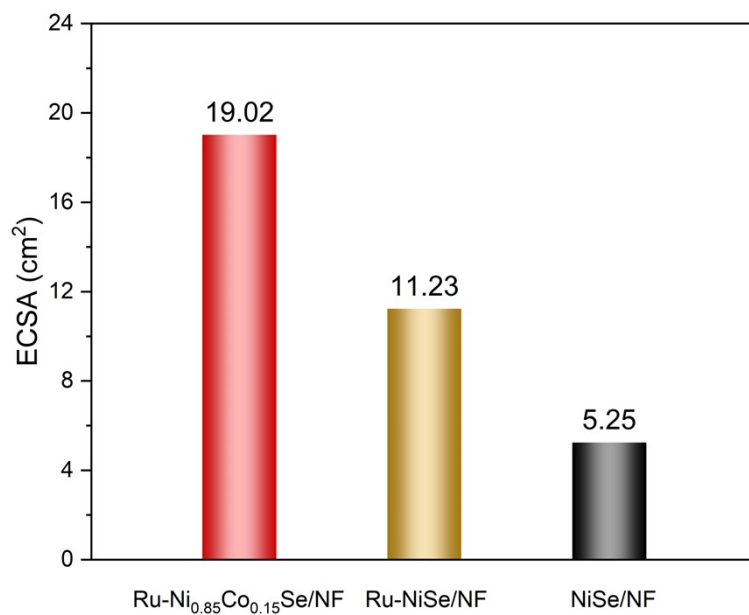


Figure S16. Electrochemical active surface area of different catalysts for HER.

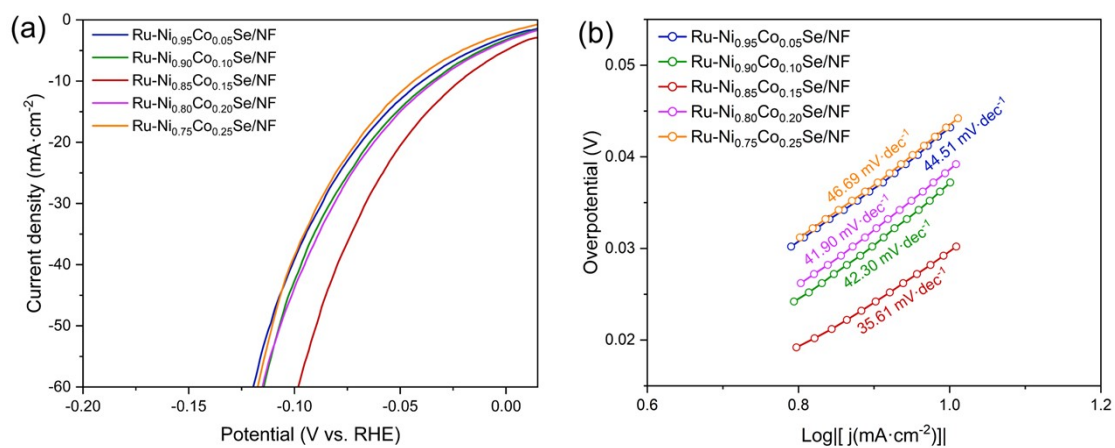


Figure S17. LSV curves and Tafel plots of different electrocatalysts in 1.0 M KOH.

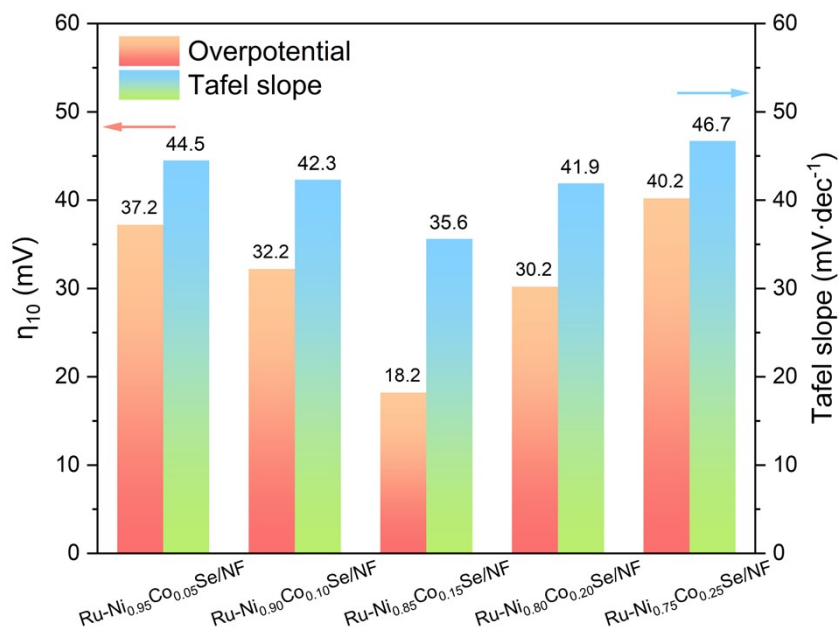


Figure S18. η changes at $10 \text{ mA}\cdot\text{cm}^{-2}$ and Tafel slope.

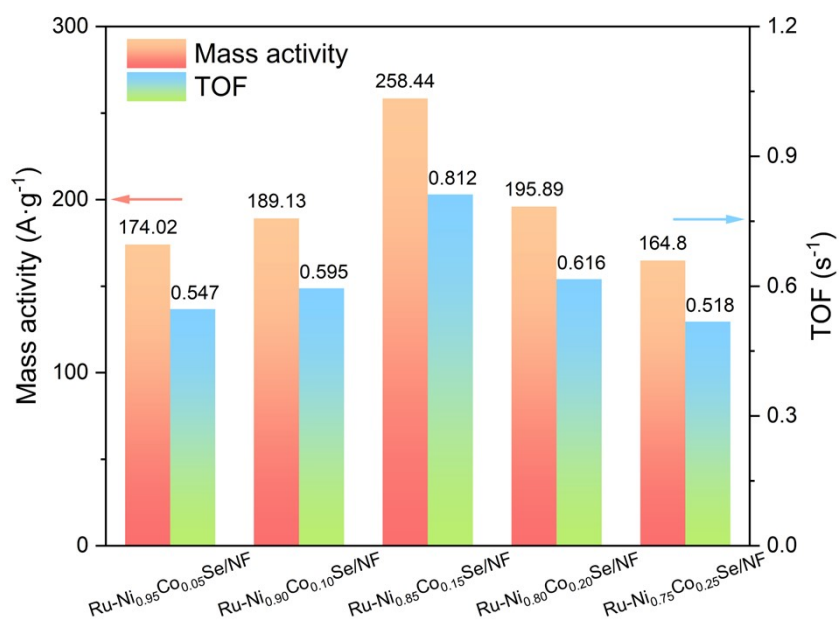


Figure S19. Mass activity and TOF of different catalysts in 1.0 M KOH.

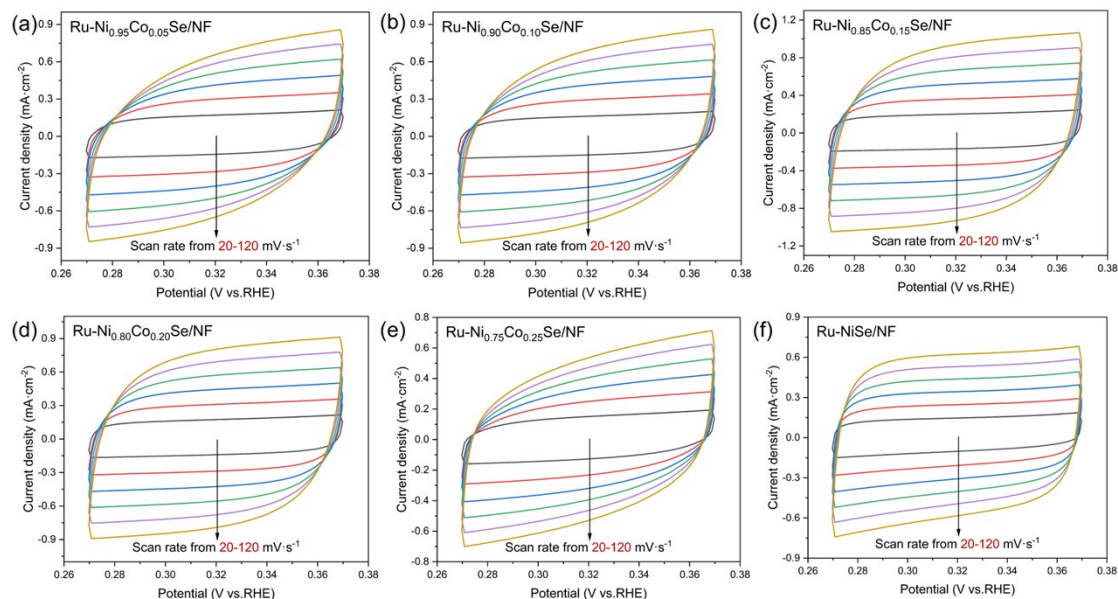


Figure S20. Cyclic voltammograms of (a)-(f) Ru-Ni_{0.95}Co_{0.05}Se/NF, Ru-Ni_{0.90}Co_{0.10}Se/NF, Ru-Ni_{0.85}Co_{0.15}Se/NF, Ru-Ni_{0.80}Co_{0.20}Se/NF, Ru-Ni_{0.75}Co_{0.25}Se/NF and Ru-NiSe/NF electrocatalysts in 1.0 M KOH at various scan rates.

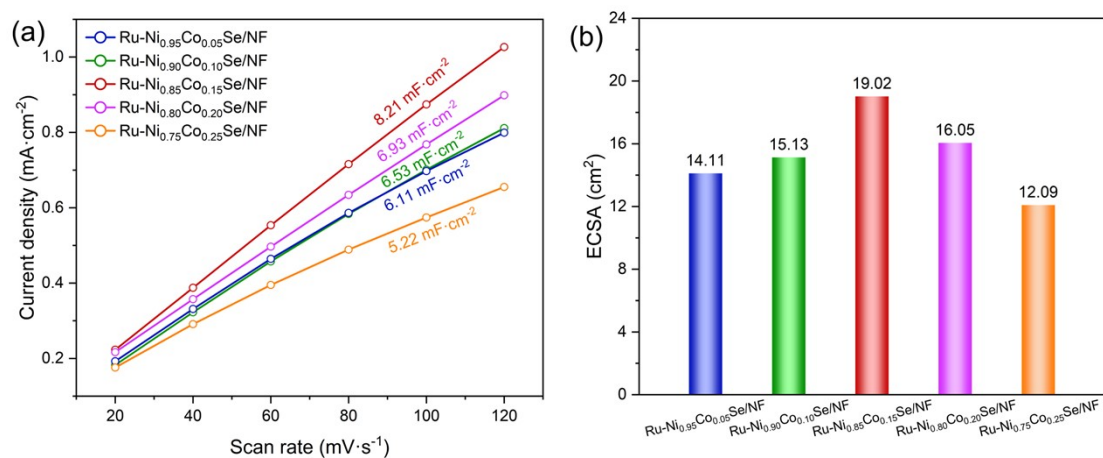


Figure S21. (a) The double-layer capacitance (C_{dl}) of different electrocatalysts. (b) Electrochemical active surface area of different catalysts for HER.

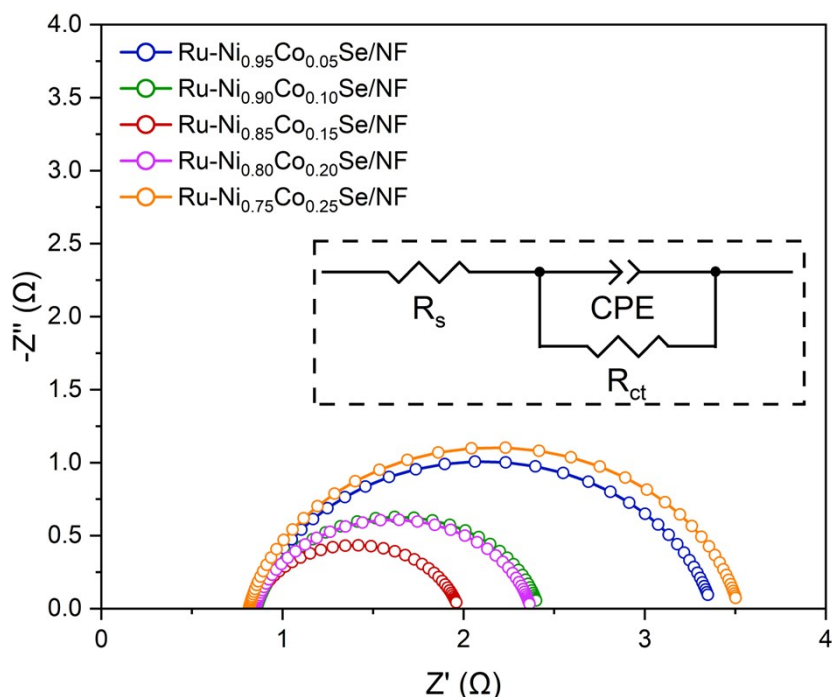


Figure S22. Nyquist plots of Ru-Ni_{0.95}Co_{0.05}Se/NF, Ru-Ni_{0.90}Co_{0.10}Se/NF, Ru-Ni_{0.85}Co_{0.15}Se/NF, Ru-Ni_{0.80}Co_{0.20}Se/NF and Ru-Ni_{0.75}Co_{0.25}Se/NF for HER.

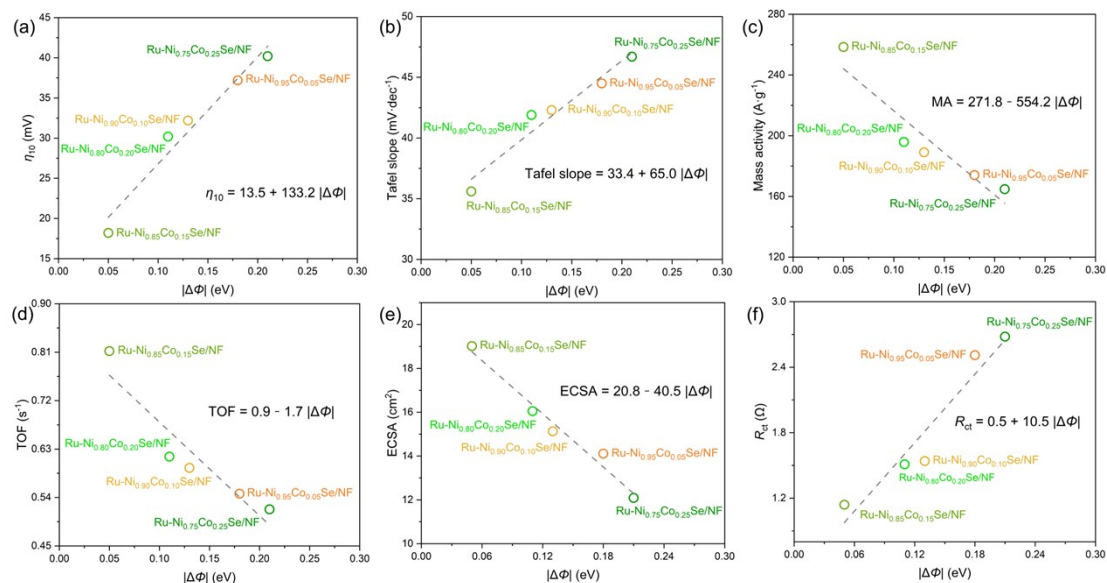


Figure S23. Plots of (a) η_{10} , (b) Tafel slope, (c) Mass activity, (d) TOF, (e) ECSA and (f) R_{ct} values as a function of the $|\Delta\Phi|$.

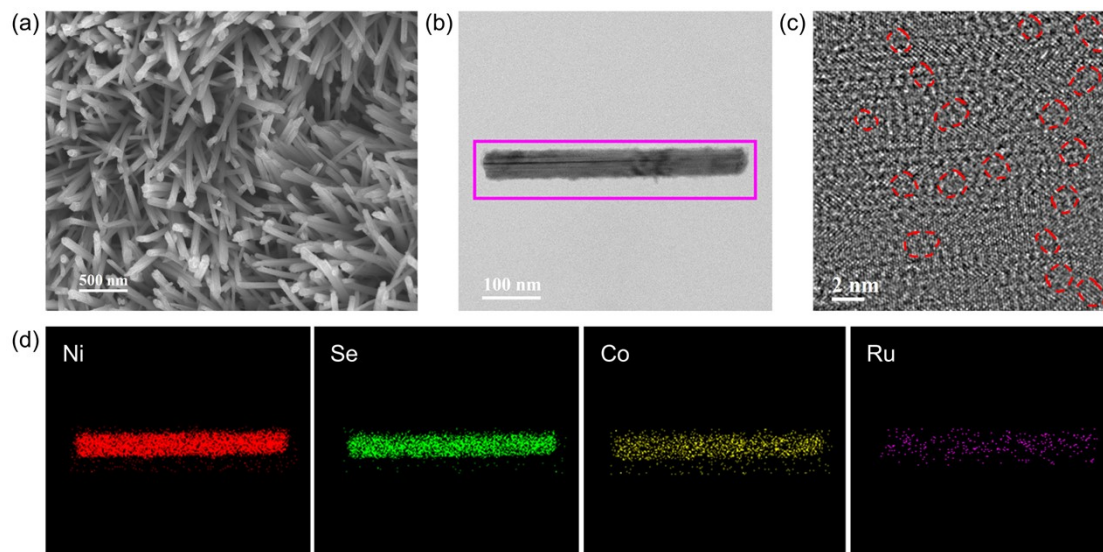


Figure S24. TEM images of Ru-Ni_{0.85}Co_{0.15}Se/NF after the stability test.

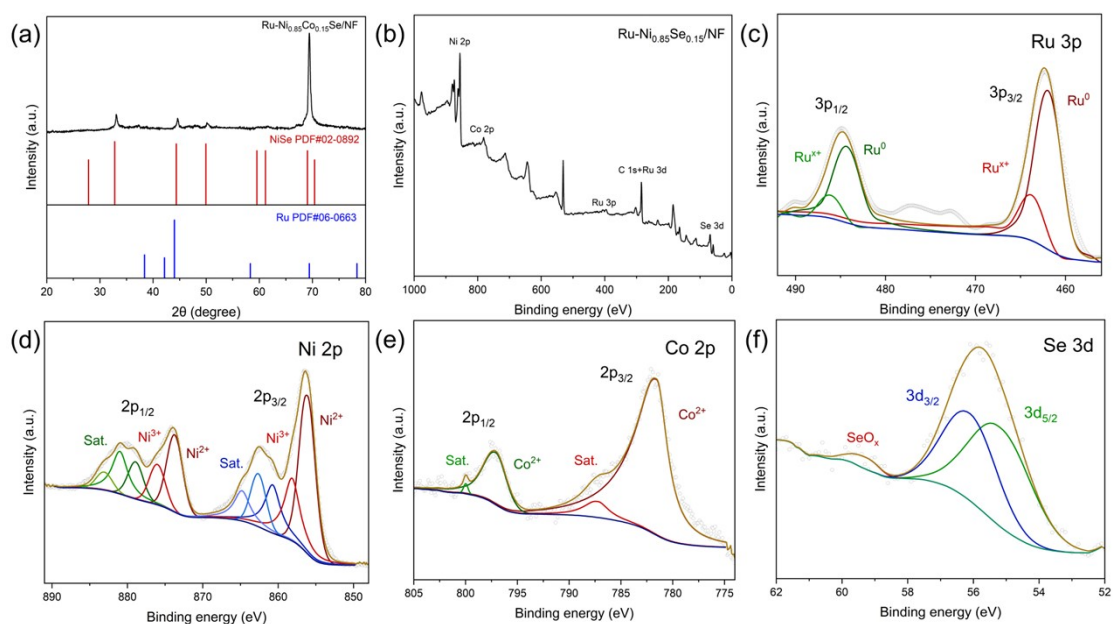


Figure S25. (a) XRD patterns of the Ru-Ni_{0.85}Co_{0.15}Se/NF after long-term stability test. XPS spectra of (b) survey spectra, (c) Ru 3p spectra and fitting curves, (d) Ni 2p spectra and fitting curves, (e) Co 2p spectra and fitting curves and (f) Se 3d spectra and fitting curves for Ru-Ni_{0.85}Co_{0.15}Se/NF after long-term stability test.

Table S1. HER performance of Ru-Ni_{0.85}Co_{0.15}Se/NF and other comparative samples in 1.0 M KOH media solution.

Electrocatalysts	η_{10} (mV)	Tafel slope (mV·dec ⁻¹)	C_{dl} (mF·cm ⁻²)	ECSA (cm ²)	R_{ct} (Ω)
NiSe/NF	93.2	107.83	2.27	5.26	5.182
Ru-NiSe/NF	54.2	70.58	4.85	11.23	3.209
Ru-Ni _{0.95} Co _{0.05} Se/NF	37.2	44.51	6.53	15.13	2.542
Ru-Ni _{0.90} Co _{0.10} Se/NF	24.0	41.90	6.11	14.11	1.561
Ru-Ni _{0.85} Co _{0.15} Se/NF	18.2	35.61	8.21	19.02	1.142
Ru-Ni _{0.80} Co _{0.20} Se/NF	30.2	42.30	6.93	16.05	1.516
Ru-Ni _{0.75} Co _{0.25} Se/NF	40.2	46.69	5.22	12.09	2.707

Table S2. HER performance of different catalysts in 1.0 M KOH media solution.

Electrocatalysts	η_{10} (mV)	Tafel slope (mV \cdot dec $^{-1}$)	Reference
Ru-Ni_{0.85}Co_{0.15}Se/NF	18.20	35.61	This work
Ru@Ni-MOF	22.00	40.00	Angew. Chem. Int. Ed. 60 (2021) 22276–22282.
Ru MNSs	24.00	33.80	Angew. Chem. Int. Ed. 61 (2022) e202116867.
Ru/np-MoS ₂	30.00	31.00	Nat. Commun. 12 (2021) 1687.
Ru/Co ₃ O ₄ NWs	30.98	69.75	Nano Energy. 85 (2021) 105940.
Ru-NiCo ₂ S ₄	32.00	41.30	Adv. Funct. Mater. 2022, 32, 2109731.
NiRu _{0.13} -BDC	34.00	32.00	Nat. Commun. 12 (2021) 1369.
Ru-MnFeP/NF	35.00	36.00	Adv. Energy Mater. 2020, 10, 2000814.
V _O -Ru/HfO ₂ -OP	39.00	29.00	Nat. Commun. 13 (2022) 1270.
Ru SAs/N-Mo ₂ C NSs	43.00	38.67	Applied Catalysis B: Environmental. 277 (2020) 119236.
Ru ₁ CoP/CDs	51.00	73.40	Angew. Chem. Int. Ed. 60 (2021) 7234–7244.
Ru _{0.10} @2H-MoS ₂	51.00	64.90	Applied Catalysis B: Environmental. 298 (2021) 120490.